Liquid-Phase Exfoliation of Biochars in Green Solvents and Correlation with Solvent Parameters

Juliana L. Vidal[a] <jlvidal@mun.ca>, Stephanie M. V. Gallant[a] <smg561@mun.ca>, Douglas D. Richards[b] <d.douglasrichards@gmail.com>, Stephanie L. MacQuarrie*[a,b] <stephanie_macquarrie@cbu.ca>, and Francesca M. Kerton*[a] <fkerton@mun.ca>

[a] Department of Chemistry, Memorial University of Newfoundland, St. John's – NL, A1B 3X7, Canada, E-mail: fkerton@mun.ca

[b] Department of Chemistry, Cape Breton University, Sydney – NS, B1P 6L2, Canada, E-mail: stephanie_macquarrie@cbu.ca

ABSTRACT

Liquid-phase exfoliation (LPE) is a process frequently used to yield small sheets of layered materials. These materials are prepared via direct or indirect sonication in an ideal solvent, and the sheets produced often present remarkable chemical and physical properties. Unfortunately, the preferred solvents for exfoliation processes are frequently toxic and possess several health risks. In this work, we show the use of LPE in green solvents to access nanostructures of biochar. Biochar is a material produced after thermochemical treatment of biomass residues and it is an important tool for the sequestration of greenhouse gases. Herein, hardwood and softwood biomass residues (e.g. sludge, bark, and sawdust) are used to prepare pristine and oxidized biochars which are then exfoliated in a range of solvents. Stable dispersions containing up to 75% by weight of exfoliated biochar could be obtained. A range of solvents were screened for LPE of biochars to identify 'green' options that could afford highly concentrated dispersions. The properties of the biochar before and after exfoliation were evaluated using Raman spectroscopy and Transmission Electron Microscopy. Correlations between effective LPE of biochar in a solvent and different solvent parameters were established. For example, LPE of oxidized biochars is more efficient in hydrogen-bond accepting solvents due to the increased concentration of carboxylic acid and alcohol functional groups within this material, when compared with pristine biochars.

INTRODUCTION

Biochar is a renewable carbon-based material produced from the thermal degradation of biomass under low supplies of oxygen via a technique known as pyrolysis.[1] Pyrolysis of waste biomass is considered to be a cost-efficient and sustainable process, because carbon dioxide (CO_2) is fixed by green plants during their photosynthesis, removed from the carbon cycle and can then be stored for centuries in the form of biochar.[1, 2] Pyrolysis also prevents the further release of greenhouse gases (e.g. methane and CO_2) during waste biomass decay at processing sites or on the forest floor. Therefore, large-scale applications of biochar could play a role in diminishing CO_2 concentrations in the atmosphere, and in mitigating climate change effects, as has been described by others previously.[2, 3] It is estimated that storing carbon in the form of biochar could potentially avoid the emission of 0.1 – 0.3 billion tons of CO_2 per year.[2]

The structure of biochar is known to be inherently amorphous (i.e. mostly sp^3 carbons in an extended network), but contains some crystalline areas composed of graphene-like sheets (i.e. sp^2 carbons) cross-linked randomly.[1, 3] Although the large-scale production and utilization of biochar is sustainable and possesses several advantages, the application of this carbon-based material is limited due to the variability and complexity of its molecular-level structure. This structure is dependent on the nature of the feedstock and pyrolysis conditions employed.[3, 4] As a consequence, this economic, environmentally-benign, and easily produced carbon material has been mainly used for soil remediation and pollutant removal,[1, 3] whereas in our opinion there is significant scope for its application in higher value fields. Expansion of biochar applications towards advanced materials is essential in society's transition towards a bio-based economy. To this end, we have recently reported the use of functionalized biochars as catalysts for the synthesis of cyclic carbonates.[5]

Exfoliation is a process through which nano- or atomic sheets can be obtained from layered precursors and can improve materials applications by revealing their inherent nanostructure and enhancing their chemical and physical properties.[6, 7] New materials created via exfoliation methods show diverse and innumerous promising applications in photovoltaic or thermoelectric devices, as electrodes for supercapacitors or batteries, and as reinforcing or conductive polymer composites.[8-14] The exfoliation of materials can be achieved using techniques such as chemical vapor deposition, intercalation, and micromechanical cleavage, but drawbacks associated with scalability, high-cost, complexity, or sensitivity to ambient conditions limit the applications of these processes.[15, 16] Liquid-phase exfoliation (LPE) was notably introduced to produce graphene from graphite,[17] and has emerged as a powerful technique to overcome some of the limitations of other processing methods. During LPE, the bulk material is immersed in an appropriate solvent and

directly or indirectly sonicated (Figure 1). [18] Sonochemical procedures are often seen as greener alternatives to those performed under classical conditions since they can save energy, generate less waste, and use less hazardous reagents.[19]

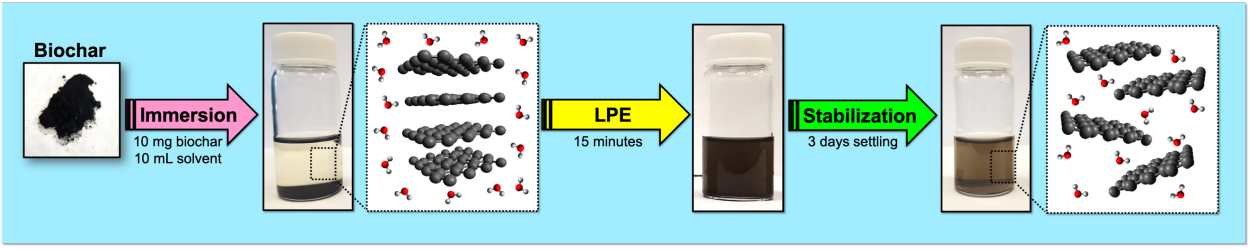

Figure 1 – Schematic diagram describing the liquid-phase exfoliation (LPE) process for biochar. Efficient and preferred solvents minimize the energy requirement of the process and stabilize the produced nanosheets.

In the initial LPE work on graphite,[17] the amount of carbonaceous material dispersed in the solvent system was shown to be directly related to the densities (ρ) and surface tensions (γ) of the solvents used. It was proposed that ideal values of ρ and γ could minimize the interfacial tension between the material and the solvent, thus decreasing the necessary energy to separate the nanosheets, and stabilize the exfoliated material against reaggregation[15-17, 20] However, this surface-matching aspect could not explain some of the divergences observed in the exfoliation of other materials. Therefore, solvent parameters such as the Hildebrand and Hansen solubility parameters, which can evaluate the interactions between solvent and material, were used to aid in the explanation of the liquid-phase processing in later studies.[21, 22] Information that can be obtained from the Hildebrand solubility parameters is somewhat limited because they are only applicable to nonpolar systems.[23] Hansen solubility parameters (HSP) have been widely used to study the solubility of polymers in different solvents. However, even the HSP cannot fully describe or predict the best solvents for the liquid-phase processing.[7, 21, 22, 24] Kamlet-Taft solvatochromic parameters are considered the most extensive and useful parameters for the investigation and understanding of solvation effects, [25, 26] and yet, as far as we are aware, they have never been used to describe the interaction between solvents and nanostructures of relevance to LPE processes. Therefore, the nature of molecular level solvent-nanostructure interactions such as hydrogen-bonding that would surely play an important role in stabilizing nanosheets currently is unclear.

Although LPE is probably the most versatile exfoliation technique for accessing dispersed nanosheets for further application and modification, the preferred solvents usually possess

several health risks, as discussed in more detail below. It is worth noting that deionized water has been employed with some success via the use of stabilizers (e.g. surfactants) or strict control of the ultrasound bath temperature and long processing times (e.g. 60 h) to yield nanosheets from layered materials.[18, 27] With respect to biochar, exfoliation has been achieved using LPE, [28-30] as well as mechanochemical techniques[31, 32] and chemical pre-treatment of biomass. [33, 34] So far, the identification of high-performance solvents for LPE of biochar has not been studied. Therefore, only preliminary assessments regarding the solvent parameters and their influence on the exfoliation of biochar have been made, and biochar samples have typically been exfoliated in a reproductive toxicant solvent (N-methyl-2-pyrrolidone) or with very low yields in water.[28-30] An increased knowledge of the effects that the solvent properties and the nature of the biomass feedstock have on the efficiency of exfoliation can further improve our understanding of biochar's structure, promote the study of new sustainable and effective alternative solvents for LPE, and improve biochar applications as an environmentally benign advanced material. Therefore, we decided to pursue an in-depth investigation of biochar exfoliation, and identify green, benign, and high-performance solvents for the liquid-phase processing of this carbon material.

EXPERIMENTAL

Synthesis and characterization of pristine and functionalized biochars. Pristine biochars **(bc)** were prepared from hardwood and softwood residues as described previously.[35] The oxidized analogues **(ox-bc)** were obtained after reaction of pristine biochars (3 g) with nitric acid (7 mol/L) at 90 °C for 3 h. Samples were washed with deionized water until neutral pH and then dried in the oven at 100 °C overnight.[36] The characterization of the obtained materials via IR spectroscopy, thermogravimetric analysis (TGA), and elemental analysis (EA) has been reported in our previous work.[5] To further assess surface functionality, Boehm titrations were performed,[37,38] showing an increase in the number of acidic sites (n_{CSF}) on the surface of oxidized biochar (from 3.84 mmol/g in pristine biochar to 4.88 mmol/g after oxidation).

Biochar dispersion procedure. 10 mL of a solvent (purchased from Sigma-Aldrich or Fischer Scientific) was added to a vial containing 10 mg of biochar or oxidized biochar from different biomass feedstocks. Samples were directly sonicated for 15 min (Misonix S-4000 Sonicator, amplitude setting = 50%). Solvents used for this procedure included: acetone; benzonitrile (BN); 1-butanol; ε-caprolactone (ε-CL); chloroform ($CHCl_3$); cyclohexanone; Cyrene®; 1,2-dichlorobenzene (1,2-DCB); dichloromethane (CH_2Cl_2); dimethyl carbonate (DMC); D-limonene; N,N-dimethylacetamide (DMA); N,N-dimethylformamide (DMF); dimethyl sulfoxide (DMSO);

ethanol; ethylene glycol (EG); ethyl acetate (EtOAc); ethyl lactate; glycerol formal (GF) hexafluorobenzene (C_6F_6); 4-methyl-2-pentanone; N-methyl-2-pyrrolidone (NMP); poly(ethylene glycol) 200 (PEG 200); poly(ethylene glycol) 400 (PEG 400); solketal; toluene; and deionized water. After sonication, black dispersions of biochar were obtained for most of the systems studied, but only a few solvents led to dispersions with significant concentrations of biochar nanostructures after allowing unstabilized materials to precipitate. The samples were allowed to settle for 3 days at ambient conditions to ensure stability, the supernatant was carefully removed, and biochar dispersed fractions were calculated via UV-Vis analysis. The dispersions were stable for at least 3 weeks. After this, minor precipitation of biochar nanosheets was observed in some cases.

UV-Vis analysis. Oxidized and pristine biochar dispersions were transferred to quartz cuvettes and analyzed using an Ocean Optics USB4000 UV-Vis spectrophotometer. A calibration curve was constructed using oxidized hardwood biochar samples in ε-CL. The biochar dispersed fractions in the samples were calculated using absorbance values at a wavelength 660 nm, following previous studies in the literature.[17, 39]

Transmission Electron Microscopy (TEM). TEM characterization of biochars before and after exfoliation in NMP were carried out at Cape Breton University, Sydney-NS, using a Hitachi HT7700 Transmission Electron Microscope containing a tungsten filament in high contract (HC) mode at 80 kV.

Raman spectroscopy. Analyses were performed using a Renishaw confocal Raman microscope with an 830 nm wavelength laser. Biochar samples before exfoliation were mounted on a quartz wafer, whereas exfoliated samples were mounted on a silicon wafer after solvent drying. Scans were performed at 0.5% or 1% laser power for 20 or 25 seconds, using a 20× optical lens. Baseline correction was implemented using a cubic spline interpolation smoothing in Renishaw's WiRE software, while peak areas and heights were calculated using a Gaussian fit in IGOR Pro software.

RESULTS AND DISCUSSION

Exfoliation of biochars. In order to find high-performance solvents for the exfoliation of biochar, including pristine (**bc**) and oxidized (**ox-bc**) biochars from different biomass feedstocks, materials were exfoliated in a wide range of different solvents (Figure S1, Supporting Information). After settling, the concentration and percentage of biochar dispersed in the supernatant was measured

using UV-Vis spectroscopy at 660 nm (Figure S2, Supporting Information).[17, 39] The molar absorptivity coefficient (α) was calculated by the linear correlation fit according to the Lambert-Beer law (Figure S3, Supporting Information). The slope of the graph of absorbance divided by cell length (A/l) as a function of biochar concentration gives a value of α = 422 L g^{-1} m^{-1}, which is considerably lower than for other works involving the exfoliation of carbon-based materials,[17, 40] but comparable to a study involving graphite exfoliation utilizing the same processing time as used herein (15 min of sonication).[39]

To identify the best solvents for LPE of biochar, we first evaluated the effect of the surface-matching aspect of the solvents in the process. We observed that the best solvents for dispersing pristine biochars from hardwood (**bc_{hw}**) and softwood (**bc_{sw}**) biomass presented high densities (ρ ~ 1.0 g/mL) and ideal surface tension values of γ ~ 20 mN/m (e.g. $CHCl_3$, CH_2Cl_2). Although ρ ~ 1.0 g/mL values were shown to lead to an effective exfoliation of the material, extremely high values were found to be detrimental to the process. When C_6F_6, the solvent with the highest density studied was used (1.62 g/mL), **bc** tended to stay on the surface forming a thin film, instead of being dispersed in the medium. This also happened when $CHCl_3$ was used to disperse **bc_{hw}**, and this difference in dispersion effect suggested that **bc_{hw}** and **bc_{sw}** must possess different chemical and physical properties, including different surface functionalities.

For the oxidized biochars from hardwood (**ox-bc_{hw}**) and softwood (**ox-bc_{sw}**) biomass, the amount of solid dispersed in the best solvents for **bc** exfoliation (e.g. $CHCl_3$, CH_2Cl_2) was negligible (< 5% by weight), and the highest levels of dispersed **ox-bc** samples were obtained in solvents with ρ ~ 1.0 g/mL and γ ~ 40 mN/m (e.g. NMP, DMSO).

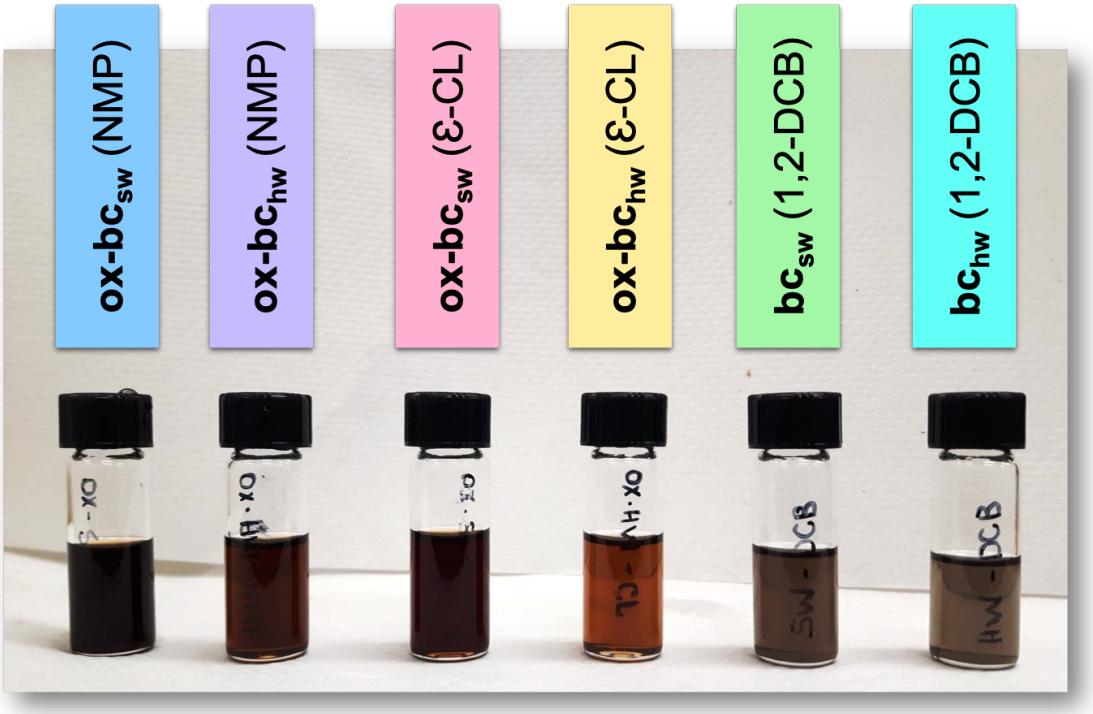

Figure 2 – Visual comparison of biochar dispersions from different feedstocks in a selection of the solvents studied.

During our studies, we observed that lower levels of dispersion were achieved for **bc$_{hw}$** and **ox-bc$_{hw}$**, when compared to **bc$_{sw}$** and **ox-bc$_{sw}$**. This difference can be seen visually in Figure 2 and in the data from UV-Vis analyses in Tables S1 and S2 (Supporting Information). This particular difference was surprising to us, because the same biochars from different waste biomass feedstocks showed very similar behaviors and gave very similar results when applied as catalysts to produce cyclic carbonates in our previous work.[5] To explain the unpredicted differences observed herein, the densities of **bc$_{sw}$** and **bc$_{hw}$** were calculated using a pycnometer. The density of **bc$_{hw}$** was found to be lower (1.02 g/mL) than **bc$_{sw}$** (1.19 g/mL), which could explain why the hardwood biochars investigated were less dispersible in the solvents studied than the softwood analogues. Besides their density, the molecular structure of biochars (i.e. the relative amounts of sp^2 and sp^3 carbons, and amount of residual oxygen from the original lignocellulosic biomass) could also have an impact in the dispersion ability observed and was therefore investigated.

Characterization of exfoliated biochars. To help to comprehend the molecular structure of biochars, LPE effects on them, and the differences observed between biochars from different feedstocks, Raman spectroscopy experiments were performed on biochars before and after

exfoliation. As shown in Figure 3, the Raman spectra of pristine as-prepared and exfoliated biochar is composed of two bands, known as G and D bands.

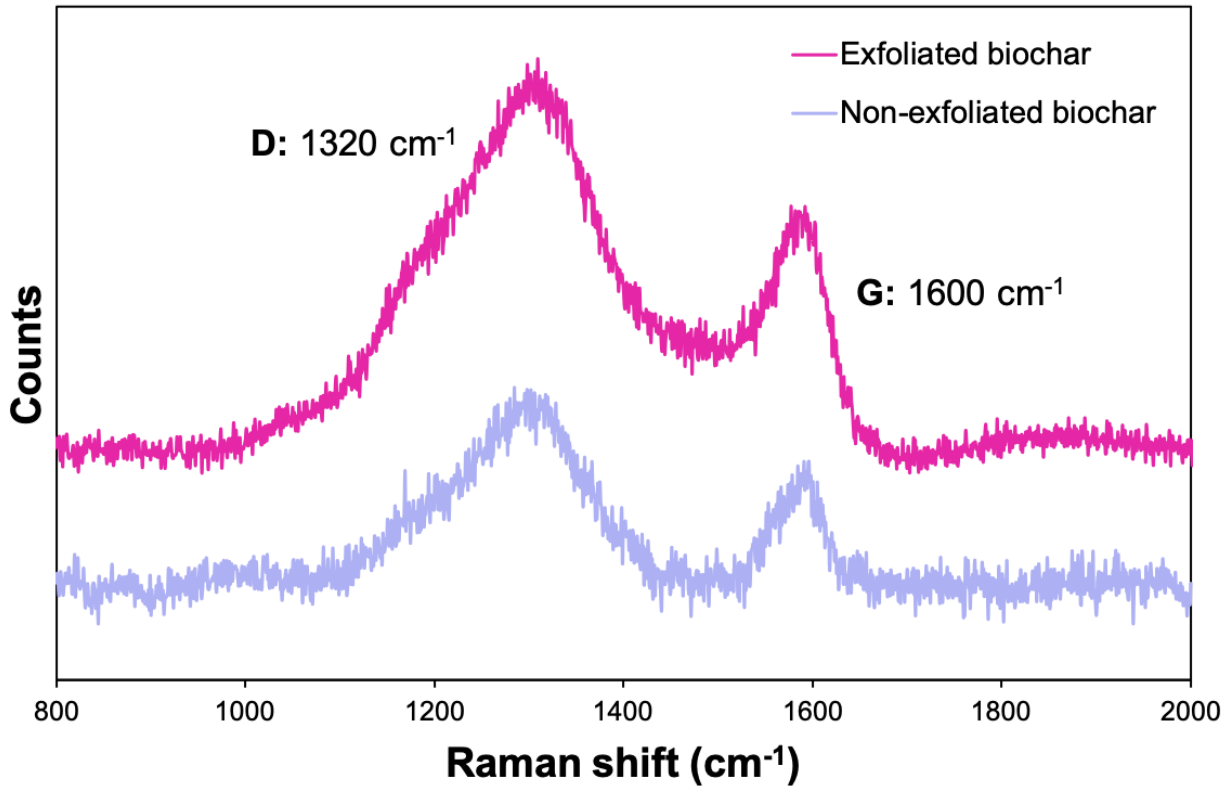

Figure 3 - Raman spectra of **bc$_{hw}$** before and after exfoliation

The G band (observed at 1600 cm^{-1}) is produced from the stretching vibrations of sp^2 carbons, whilst the D band (observed at 1320 cm^{-1}) originates from the breathing mode of hexagonal rings and it is only Raman active if the ring is close to a defect.[41, 42] Therefore, the G band indicates crystallinity or presence of graphitic arrangements, whereas the D band is related to defects or disorders of the material. The ratio between the intensity of these two bands (I_G/I_D) is known to estimate the molecular order within carbon networks.[43] In the current study, natural and exfoliated hardwood biochar samples present a higher I_G/I_D ratio when compared to the softwood analogues, meaning an increased sp^2 carbon content and improved crystallinity (Table 1). Because graphitic structures are more ordered, dense, and rigid than the amorphous phase, they are less susceptible to exfoliation, [28,29] which explains the increased yields of exfoliated softwood biochar in all the solvents studied for LPE and the difficult in finding high-performance solvents for the processing of the more highly crystalline materials. Although density filters were used during Raman analysis to decrease the laser power and avoid potential thermal degradation of samples,

the spectra of oxidized biochars before and after exfoliation could not be obtained. We presume that, due to the existence of local functional differences (and greater molecular asymmetry), bonding vibrations and rotations in **ox-bc** might not be strong enough to provide signals in the Raman experiment or may be Raman inactive vibrations.

Table 1 – Exfoliation effects in the molecular structure of biochars from different biomass sources

Biochar type	**I_G/I_D (non-exfoliated)**	**I_G/I_D (exfoliated)**
bc_{hw}	0.45 ± 0.01	0.55 ± 0.05
bc_{sw}	0.18 ± 0.06	0.19 ± 0.01

TEM micrographs of pristine hardwood samples before and after direct sonication are presented in Figure 4. A multilayered structure of biochar is seen in samples of **bc_{hw}** before exfoliation (Figure 4A and Figure 4B), whereas nanocrystalline structures are present in the exfoliated biochar. Micrographs of the processed material show the presence of black dots, representing aromatic clusters (Figure 4C). These consist of two- or more multi-layered graphene-like nanosheets turbostatically ordered (i.e. layers not aligned).[28] Nanocrystalline stripes could also be observed in the structure of exfoliated biochar, as well as the presence of atomic arrangements at the edges of the dispersed material (Figure 4D). The presence of aromatic clusters, nanocrystalline stripes, and atomic arrangements in the structure of exfoliated biochar observed via TEM demonstrate the value of LPE in gaining access to the nanostructures of this biorenewable material. The morphology and structures visible by TEM for **bc_{hw}** and **bc_{sw}** are similar to those seen previously rice straw biochar.[28] TEM micrographs of the remaining biochars studied (**ox-bc_{hw}, ox-bc_{sw},** and **bc_{sw}**) before and after treatment using ultrasound are shown in Figure S4 (Supporting Information).

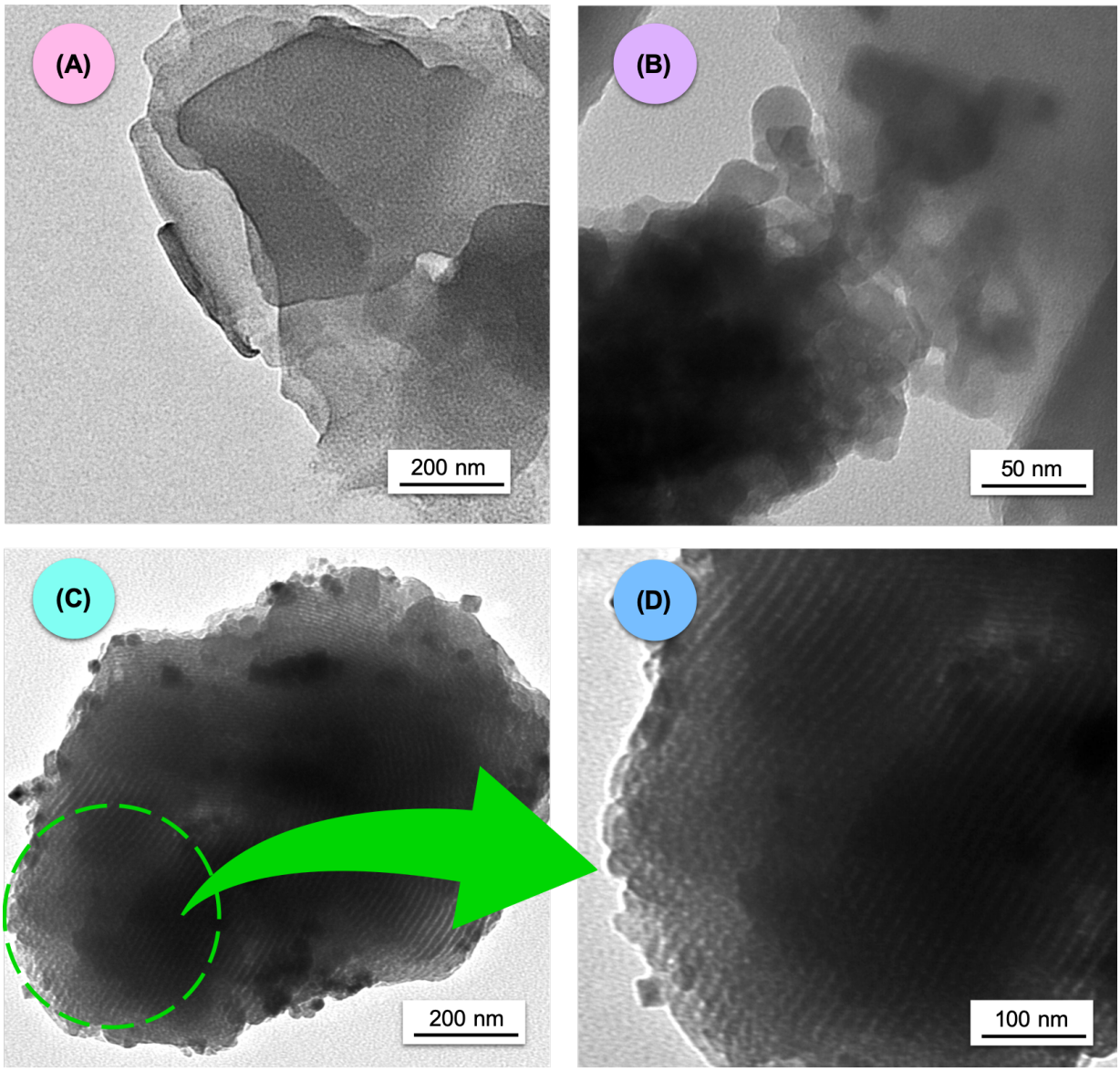

Figure 4 - TEM micrographs of hardwood biochar (**bc$_{hw}$**) samples. Figures (A) and (B) show the layered structure of **bc$_{hw}$** before exfoliation, whereas aromatic clusters (i.e. black dots) and nanocrystalline stripes are observed after biochar exfoliation in Figure (C). Atomic arrangements can be observed at the edges of the exfoliated material and are further highlighted in Figure (D).

Green solvents for biochar exfoliation. Based on our preliminary studies that identified the ideal values of surface tension (γ) and density (ρ) of solvents for LPE of pristine and oxidized biochars, an attempt to explore the nature of biochar exfoliation and an assessment regarding the greenest solvents for the processing was realized.

In Tables S1 and S2 (Supporting Information), a correlation between solvent parameters and percentage of **bc** and **ox-bc** dispersed in the samples during LPE can be seen. Reproducibility

was assessed by performing exfoliations in triplicate. As expected, the evaluation of LPE using only the surface-matching aspect (i.e. density and surface tension) was superficial, and the contribution of biochar-solvent interactions is also needed. Aware of the well-known limitations of Hildebrand's solubility parameters (e.g. only applicable for nonpolar systems), Hansen solubility parameters (HSP) and their effects in biochar exfoliation were assessed. HSP have been extensively used to aid in the selection of solvents in coating industries and to predict solvent-polymer compatibility.[21, 44] Each substance can be described using three HSP, which are related to the energy from dispersion forces (δ_D), dipolar intermolecular forces (δ_P), and hydrogen bonds (δ_H) between molecules.[44] When HSP of the solvent and solute are similar, they usually show a high affinity for each other and are likely to mix easily to form a solution. One might expect similarities between the solvent and materials' surface functionality to similarly aid in dispersion processes. Some of the solvents able to disperse **bc** and **ox-bc** had HSP values in the following ranges: δ_D ~ 17 $MPa^{1/2}$, δ_H ~ 7 $MPa^{1/2}$, δ_P ~ 6 $MPa^{1/2}$ (average values for CH_2Cl_2 and ethyl acetate) and δ_D ~ 17 $MPa^{1/2}$, δ_H ~ 20 $MPa^{1/2}$, δ_P ~ 11 $MPa^{1/2}$ (average values for glycerol formal and ethylene glycol). However, some solvents with HSP values out of the ideal ranges were also able to exfoliate **bc** and **ox-bc.** For example, δ_H = 0 and δ_P = 0 for C_6F_6 and this solvent was effective in LPE. Other examples of effective LPE solvents outside the two typical HSP ranges included benzonitrile, solketal, PEG 200, PEG 400, and ε-CL (Tables S1 and S2, Supporting Information). Therefore, even though HSP were used by others previously to evaluate the nature of exfoliation of materials, [39, 40] they could not effectively describe the LPE of biochar because a direct, regular, and predictable relationship between the high-performance solvents for biochar exfoliation and δ_D, δ_H, δ_P values could not be obtained.

Kamlet-Taft solvatochromic parameters are the most extensively used quantitative measure of solvent characteristics and solvent-solute interactions, which can be explained in terms of three properties, α, β, and π^*.[25, 45] The parameter α quantifies the ability of the solvent to donate a hydrogen-bond, β describes its ability to accept a hydrogen-bond, and π^* represents its polarity/polarizability, which reflects the solvent's ability to stabilize a charge or a dipole.[26] Most solvents present values between 0 and 1 on each scale.

Although the Kamlet-Taft solvatochromic parameters have been widely utilized in the investigation of diverse solvent-solute systems, to the best of our knowledge, they have not been applied to explore the nature of LPE of materials. For those reasons, we decided to study if there was any correlation between the percentage of biochar dispersed in our samples and α, β, and π^* values of the solvents used. As shown in our preliminary studies and in Table S1 (Supporting

Information), good dispersions of pristine biochar (**bc**) nanosheets could be obtained in solvents with ρ ~ 1.0 g/mL and γ ~ 20 mN/m. However, solvents with γ values far from the ideal could also successfully disperse biochar samples. Examples of these exceptions include (with γ values in parentheses): deionized water (72 mN/m); BN (39 mN/m); 1,2-DCB (37 mN/m); NMP (40 mN/m); and solketal (32 mN/m). A better understanding of these results can be obtained by looking at their Kamlet-Taft parameters: all effective solvents for **bc** dispersion with non-ideal γ values had $\pi^* \geq 0.50$. This observation indicated that solvatochromic parameters could help to explain the nature of biochar exfoliation: solvents with high polarity/polarizability values (i.e. high values of π^*) could interact more effectively with the electron cloud generated by the graphene-like sheets within the biochar structure, as it can be seen in Figure 5.

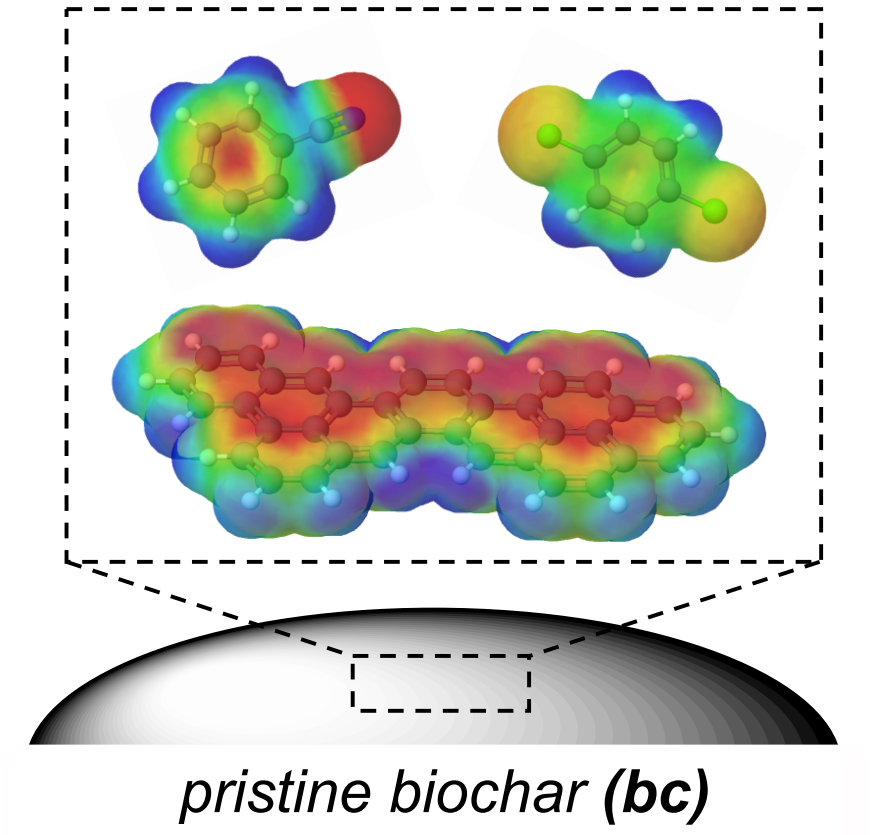

Figure 5 – Proposed interactions between **bc** and solvents with high polarity/polarizability.

Since LPE of oxidized biochar (**ox-bc**) exfoliation was not possbile in some of the solvents that worked for **bc** exfoliation (e.g. with high values of π^*, but low values of α and β), **ox-bc** processing was found to be dependent on different solvent parameters. From the results in Table S2 (Supporting Information), we observed that there were two classes of solvents that could produce **ox-bc** nanosheets via LPE: Solvents with ρ ~ 1.0 g/mL and γ ~ 40 mN/m, and if the

surface energies were different to these, solvents with β values ≥ 0.50 were also able to stabilize dispersions effectively. We propose that solvents with good hydrogen-bonding acceptor ability (i.e. high β values) are able to interact more effectively with the hydroxyl and carboxyl groups on the surface of the oxidized biochar (Figure 6), and this correlates well with the increased acidity of the surface of **ox-bc** as characterized via Boehm titrations.

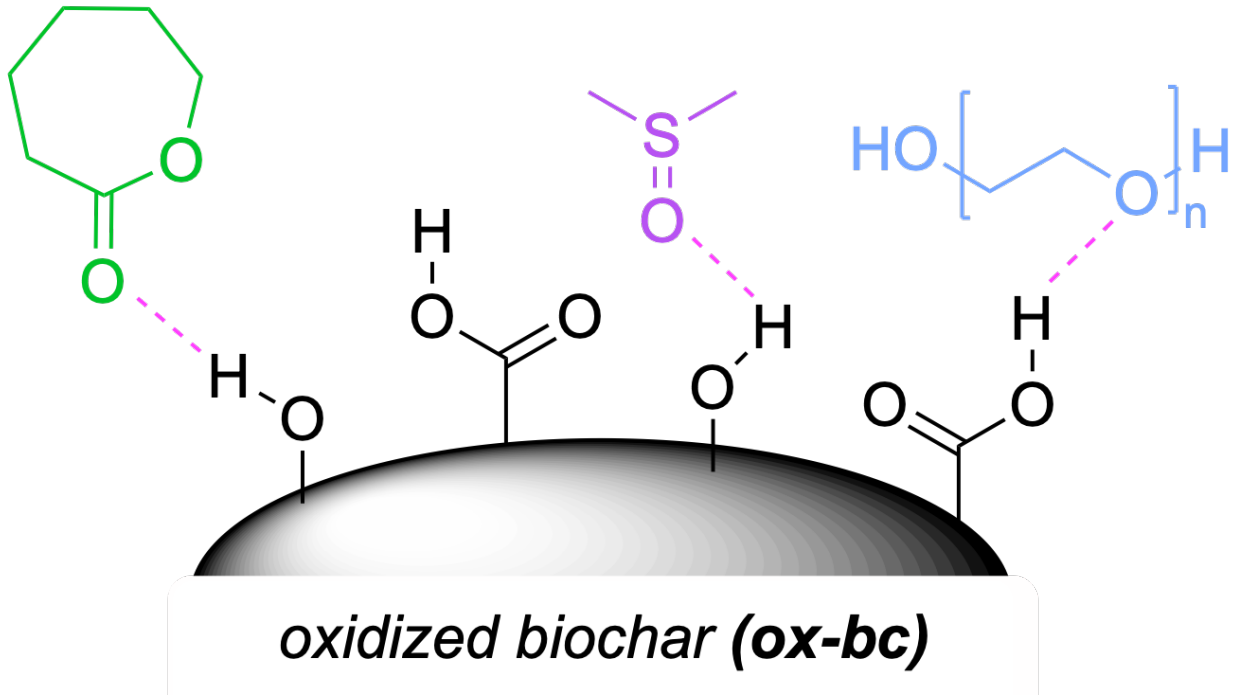

Figure 6 – Proposed interactions between **ox-bc** and solvents with hydrogen-bond acceptor solvents

Although several of the high-performance solvents evaluated for the production of biochar nanostructures had desirable characteristics for LPE (e.g. high levels of dispersion achieved and low-boiling points), their use in scaled-up processing would be limited due to their significant toxicity levels. Chloroform, dichloromethane, and 1,2-dichlorobenzene are able to disperse more than 20% **bc** by weight, but are toxic and suspected human carcinogens according to the International Agency for Research on Cancer (IARC).[46-48] Solvents such as acetone, ethyl acetate, dimethyl carbonate, solketal, and even deionized water can disperse around 10% **bc** by weight using only 15 minutes of sonication. These solvents are considered green alternatives due to their low toxicity and high biodegradability, as indicated by various solvent selection guides.[49-51] Dimethyl carbonate can also be derived from carbon dioxide, contributing to the storage, usage, and transformation of this greenhouse gas.[51]

Different observations and correlations could be made for LPE of **ox-bc**. Nanostructures of **ox-bc** could be obtained in solvents typically used for exfoliation of layered materials such as N-methyl-2-pyrrolidone (NMP) and dimethyl sulfoxide (DMSO) via LPE. However, in the current study, ethylene glycol and poly(ethylene glycols) (PEGs 200 and 400) could exfoliate more than 40% **ox-bc** by weight due to their ideal surface tensions combined with their excellent of hydrogen-bonding acceptance ability (β). PEGs, although polymeric, provide excellent green liquid environments for LPE, since they are biodegradable, biocompatible, and nontoxic low molecular weight polymers, with low flammability and vapor pressure.[52] They are widely used in consumer products, and are approved for internal consumption by the US Food and Drug Agency.[52] Ethylene glycol (EG) can be considered a less desired alternative when compared to PEGs for the exfoliation of **ox-bc,** since high doses can be toxic to humans and aquatic biota upon ingestion or exposure.[53] However, EG can be produced sustainably from lignocellulosic biomass, sugars, bacteria, and algae.[54] Although ε-caprolactone (ε-CL) has a lower surface tension value when compared to EG, PEG 200, and PEG 400, it can disperse more than 20 % **ox-bc** by weight. ε-CL can cause eye irritation, but overall is considered a nontoxic, affordable, and important commodity chemical for the production of the biodegradable poly(ε-caprolactone).[55] It is not widely used as an ester solvent unlike more volatile esters such as EtOAc. A comparison of selected solvents (green and traditional) for LPE of **bc** and **ox-bc** is presented in Figure 7. Based on the diagram, we can observe that under the conditions explored **ox-bc** generally achieves higher levels of dispersion (up to 75 % by weight) when compared to **bc** (up to 51% by weight). This is likely due to the hydrogen-bond donating ability of the functional groups on the surface of **ox-bc**.

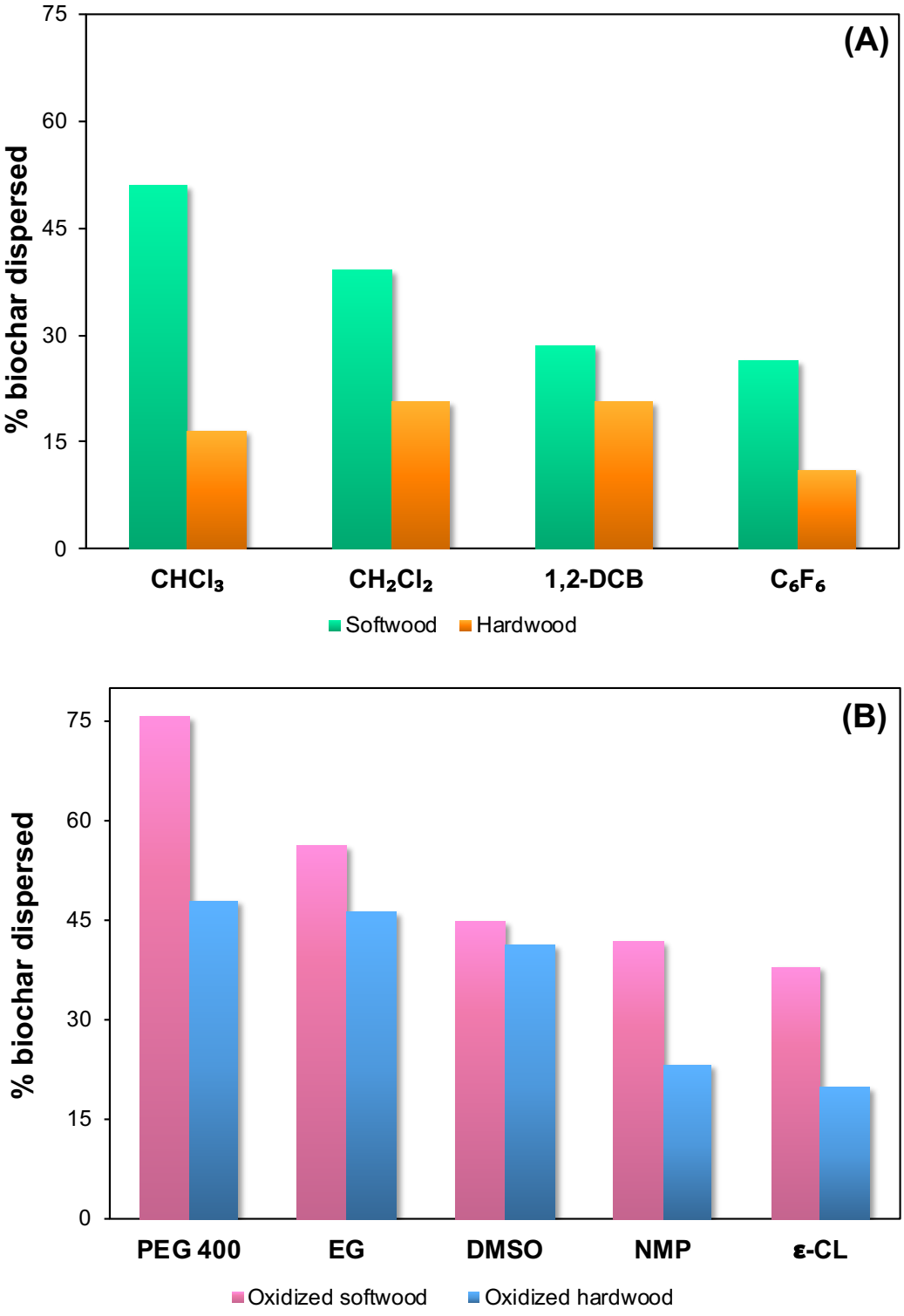

Figure 7 – Percentage by weight of biochar dispersed in samples of (A) **bc** and (B) **ox-bc** in different solvents

Effect of sonication time on the liquid-phase exfoliation of biochar. After the investigation of green environments for the LPE of biochar, **bc$_{hw}$** samples were sonicated for 15, 30, 60, 90, and 120 min in ethyl acetate, in order to evaluate the influence of time on the process. The procedure was performed in triplicate. The weight percent **bc** dispersed in the samples was found to increase gradually, as it can be seen in Figure 8.

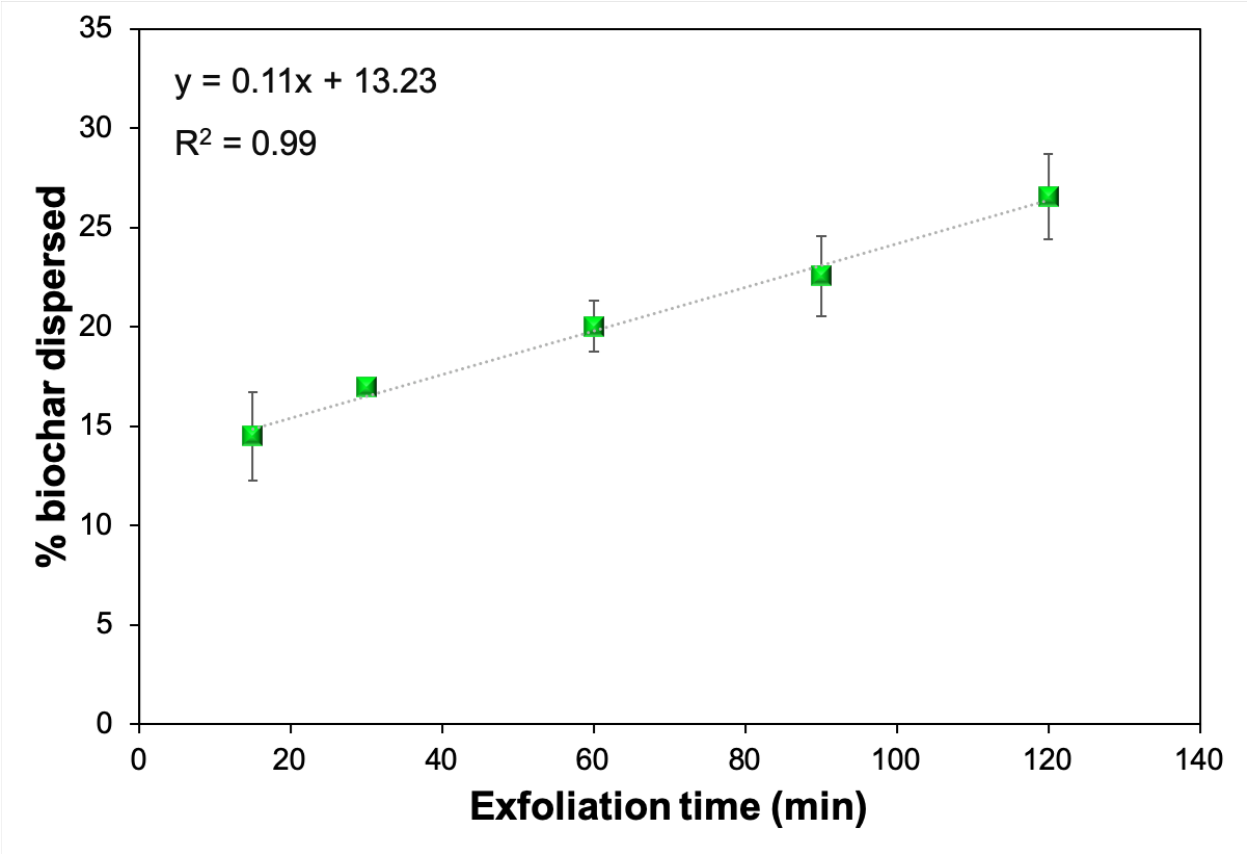

Figure 8 – Percentage by weight of exfoliated **bc$_{hw}$** as a function of exfoliation time in ethyl acetate, showing a linear behavior and following the equation y = 0.11x + 13.23

Although the yield of nanostructures dispersed in the medium increases with sonication time, the quality of the exfoliated material can decrease during longer LPEs, and the use of viscous solvents is often required to stabilize and preserve the obtained dispersions.[39] The quality of the produced biochar nanostructures after different exfoliation times was assessed via Raman spectroscopy, and I_G/I_D ratios were calculated for each processing time (Figure 9). Interestingly, there was no significant decrease in the I_G/I_D values, indicating that better yields of biochar nanostructures can be obtained herein during longer sonication times even in solvents with low viscosities.

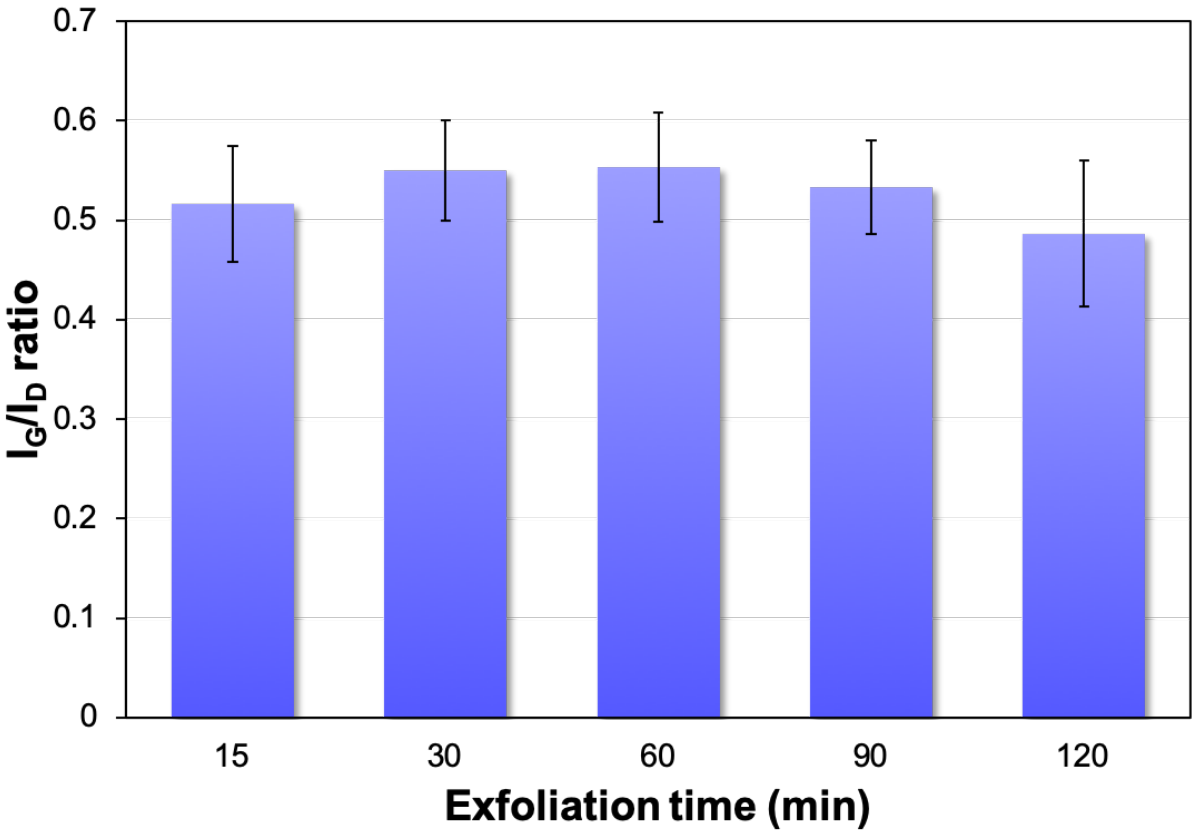

Figure 9 – I_G/I_D ratios of exfoliated **bc_{hw}** as a function of exfoliation time in ethyl acetate

CONCLUSIONS

LPE has been applied to pristine and functionalized biochars from different waste biomass feedstocks to obtain nanostructures of the respective layered materials. The nature of biochar's exfoliation was investigated to discover various green and benign liquid environments for LPE, improving future applications of the nanostructured materials. Both solvent surface-matching properties (surface tension and density) and biochar-solvent intermolecular interactions have been shown to greatly influence the process. To our knowledge, this is the first time that Kamlet-Taft solvatochromic parameters have been used to aid in understanding LPE. Solvents with ρ ~ 1.0 g/mL, γ ~ 20 mN/m or high values of π^* showed good performance in the exfoliation of pristine biochars, whereas solvents with ρ ~ 1.0 g/mL, γ ~ 40 mN/ or with good hydrogen-bond accepting ability (β) could successfully exfoliate oxidized biochars. Using only 15 min of sonication, dispersions with more than 10% by weight of pristine biochar could be obtained in green solvents including acetone, dimethyl carbonate, ethyl acetate, solketal, and deionized water, whereas significant yields of dispersed oxidized biochar nanosheets could be obtained in sustainable solvents such as ε-caprolactone, ethylene glycol, and poly(ethylene glycols) 200 and 400.

Moreover, no strict control of temperature was needed, and no surfactants were used to stabilize the dispersions. These data and reasonings will hopefully allow others to evaluate the solvents applied in LPE of other materials, employing alternatives to commonly used and toxic dipolar aprotic solvents such as NMP. The produced biochar nanostructures in the current study have large potential to be applied as reinforcing agents in polymer composites, an investigation of which will be pursued in our future work.

ACKNOWLEDGMENTS

Financial support was provided by the Natural Sciences and Engineering Research Council (NSERC), Canada Foundation for Innovation (CFI), the provincial government of Newfoundland and Labrador, and Memorial University of Newfoundland (MUN). Dr. Kelly Kawboldt (Faculty of Engineering and Applied Science, MUN) is thanked for softwood biochar samples and Dr. Erika Merschrod is thanked for access to the Raman instrumentation.

Keywords: biomass, exfoliation, nanostructures, green solvents.

REFERENCES

1. J. Lehmann and S. Joseph, *Biochar for environmental management: Science and Technology*, Earthscan, Sterling, VA, 2009.

2. D. Woolf, J. E. Amonette, F. A. Street-Perrott, J. Lehmann and S. Joseph, *Nat. Commun.*, 2010, **1**, 56-64.

3. W. J. Liu, H. Jiang and H. Q. Yu, *Chem. Rev.*, 2015, **115**, 12251-12285.

4. P. Basu, in *Biomass Gasification, Pyrolysis and Torrefaction*, Academic Press, Boston, 2nd edn., 2013, pp. 147-176.

5. J. L. Vidal, V. P. Andrea, S. L. MacQuarrie and F. M. Kerton, *ChemCatChem*, 2019, **11**, 4089-4095.

6. J. N. Coleman, M. Lotya, A. O'Neill, S. D. Bergin, P. J. King, U. Khan, K. Young, A. Gaucher, S. De, R. J. Smith, I. V. Shvets, S. K. Arora, G. Stanton, H.-Y. Kim, K. Lee, G. T. Kim, G. S. Duesberg, T. Hallam, J. J. Boland, J. J. Wang, J. F. Donegan, J. C. Grunlan, G. Moriarty, A. Shmeliov, R. J. Nicholls, J. M. Perkins, E. M. Grieveson, K. Theuwissen, D. W. McComb, P. D. Nellist and V. Nicolosi, *Science*, 2011, **331**, 568-571.

7. H. Tao, Y. Zhang, Y. Gao, Z. Sun, C. Yan and J. Texter, *Phys. Chem. Chem. Phys.*, 2017, **19**, 921-960.

8. G. Cunningham, M. Lotya, N. McEvoy, G. S. Duesberg, P. van der Schoot and J. N. Coleman, *Nanoscale*, 2012, **4**, 6260-6264.
9. R. J. Smith, P. J. King, M. Lotya, C. Wirtz, U. Khan, S. De, A. O'Neill, G. S. Duesberg, J. C. Grunlan, G. Moriarty, J. Chen, J. Wang, A. I. Minett, V. Nicolosi and J. N. Coleman, *Adv. Mater.*, 2011, **23**, 3944-3948.
10. Y. Zhu, S. Murali, M. D. Stoller, K. J. Ganesh, W. Cai, P. J. Ferreira, A. Pirkle, R. M. Wallace, K. A. Cychosz, M. Thommes, D. Su, E. A. Stach and R. S. Ruoff, *Science*, 2011, **332**, 1537-1541.
11. P. May, U. Khan, A. O'Neill and J. N. Coleman, *J. Mater. Chem.*, 2012, **22**, 1278-1282.
12. S. Pavlidou and C. D. Papaspyrides, *Prog. Polym. Sci.*, 2008, **33**, 1119-1198.
13. S. Stankovich, D. A. Dikin, G. H. B. Dommett, K. M. Kohlhaas, E. J. Zimney, E. A. Stach, R. D. Piner, S. T. Nguyen and R. S. Ruoff, *Nature*, 2006, **442**, 282-286.
14. H.-D. Huang, P.-G. Ren, J. Chen, W.-Q. Zhang, X. Ji and Z.-M. Li, *J. Membr. Sci.*, 2012, **409-410**, 156-163.
15. V. Nicolosi, M. Chhowalla, M. G. Kanatzidis, M. S. Strano and J. N. Coleman, *Science*, 2013, **340**, 1420- 1438.
16. C. Backes, T. M. Higgins, A. Kelly, C. Boland, A. Harvey, D. Hanlon and J. N. Coleman, *Chem. Mater.*, 2016, **29**, 243-255.
17. Y. Hernandez, V. Nicolosi, M. Lotya, F. M. Blighe, Z. Sun, S. De, I. T. McGovern, B. Holland, M. Byrne, Y. K. Gun'Ko, J. J. Boland, P. Niraj, G. Duesberg, S. Krishnamurthy, R. Goodhue, J. Hutchison, V. Scardaci, A. C. Ferrari and J. N. Coleman, *Nat. Nanotechnol.*, 2008, **3**, 563-568.
18. N. Wang, Q. Xu, S. Xu, Y. Qi, M. Chen, H. Li and B. Han, *Sci. Rep.*, 2015, **5**, 16764-16772.
19. M. Lancaster, *Green chemistry: An introductory text*, RSC Publishing, Cambrigde, 2002.
20. A. Ciesielski and P. Samori, *Chem. Soc. Rev.*, 2014, **43**, 381-398.
21. J. Shen, Y. He, J. Wu, C. Gao, K. Keyshar, X. Zhang, Y. Yang, M. Ye, R. Vajtai, J. Lou and P. M. Ajayan, *Nano Lett.*, 2015, **15**, 5449-5454.
22. S. D. Bergin, Z. Sun, D. Rickard, P. V. Streich, J. P. Hamilton and J. N. Coleman, *ACS Nano*, 2009, **3**, 2340-2350.
23. C. Reichardt, in *Solvents and Solvent Effects in Organic Chemistry*, Wiley-VCH, Weinhem, 3rd edn., 2003, pp. 5-56.
24. K.-G. Zhou, N.-N. Mao, H.-X. Wang, Y. Peng and H.-L. Zhang, *Angew. Chem. Int. Ed.*, 2011, **50**, 10839-10842.
25. P. G. Jessop, D. A. Jessop, D. Fu and L. Phan, *Green Chem.*, 2012, **14**, 1245-1259.
26. M. J. Kamlet, J. L. M. Abboud, M. H. Abraham and R. W. Taft, *J. Org. Chem.*, 1983, **48**, 2877-2887.

27. J. Kim, S. Kwon, D. H. Cho, B. Kang, H. Kwon, Y. Kim, S. O. Park, G. Y. Jung, E. Shin, W. G. Kim, H. Lee, G. H. Ryu, M. Choi, T. H. Kim, J. Oh, S. Park, S. K. Kwak, S. W. Yoon, D. Byun, Z. Lee and C. Lee, *Nat. Commun.*, 2015, **6**, 8294-8302.
28. X. Xiao and B. Chen, *Environ. Sci. Technol.*, 2017, **51**, 5473-5482.
29. G. Liu, H. Zheng, Z. Jiang, J. Zhao, Z. Wang, B. Pan and B. Xing, *Environ. Sci. Technol.*, 2018, **52**, 10369-10379.
30. P. Oleszczuk, W. Ćwikła-Bundyra, A. Bogusz, E. Skwarek and Y. S. Ok, *J. Anal. Appl. Pyrol.*, 2016, **121**, 165-172.
31. M. Naghdi, M. Taheran, S. K. Brar, T. Rouissi, M. Verma, R. Y. Surampalli and J. R. Valero, *J. Clean. Prod.*, 2017, **164**, 1394-1405.
32. L. Li, K. Zhang, L. Chen, Z. Huang, G. Liu, M. Li and Y. Wen, *New J. Chem.*, 2017, **41**, 9649-9657.
33. M. Genovese, J. Jiang, K. Lian and N. Holm, *J. Mater. Chem. A*, 2015, **3**, 2903-2913.
34. S. Roy, U. Kumar and P. Bhattacharyya, *Environ. Sci. Pollut. Res. Int.*, 2019, **26**, 7272-7276.
35. A. J. Carrier, I. Abdullahi, K. A. Hawboldt, B. Fiolek and S. L. MacQuarrie, *J. Phys. Chem. C*, 2017, **121**, 26300-26307.
36. Y. Gokce and Z. Aktas, *Appl. Surf. Sci.*, 2014, **313**, 352-359.
37. S. L. Goertzen, K. D. Thériault, A. M. Oickle, A. C. Tarasuk and H. A. Andreas, *Carbon*, 2010, **48**, 1252-1261.
38. J. Schönherr, J. Buchheim, P. Scholz and P. Adelhelm, *C*, 2018, **4**, 22-38.
39. H. J. Salavagione, J. Sherwood, M. De Bruyn, V. L. Budarin, G. J. Ellis, J. H. Clark and P. S. Shuttleworth, *Green Chem.*, 2017, **19**, 2550-2560.
40. L. Xu, J.-W. McGraw, F. Gao, M. Grundy, Z. Ye, Z. Gu and J. L. Shepherd, *J. Phys. Chem. C*, 2013, **117**, 10730-10742.
41. A. C. Ferrari and J. Robertson, *Phys. Rev. B*, 2000, **61**, 14095-14107.
42. C. Guizani, K. Haddad, L. Limousy and M. Jeguirim, *Carbon*, 2017, **119**, 519-521.
43. L. G. Cançado, A. Jorio, E. H. M. Ferreira, F. Stavale, C. A. Achete, R. B. Capaz, M. V. O. Moutinho, A. Lombardo, T. S. Kulmala and A. C. Ferrari, *Nano Lett.*, 2011, **11**, 3190-3196.
44. C. M. Hansen, *Hansen Solubility Parameters: A User's Handbook*, CRC Press: Taylor & Francis, Boca Raton, 2nd edn., 2012.
45. L. Crowhurst, R. Falcone, N. L. Lancaster, V. Llopis-Mestre and T. Welton, *J. Org. Chem.*, 2006, **71**, 8847-8853.
46. International Agency for Research on Cancer (IARC), *IARC monographs on the evaluation of carcinogenic risks to humans: Chloroform*, IARC, Lyon, France, 1999.

47. International Agency for Research on Cancer (IARC), *IARC monographs on the evaluation of carcinogenic risks to humans: Dichlorobenzenes*, IARC, Lyon, France, 1999.
48. International Agency for Research on Cancer (IARC), *IARC monographs on the evaluation of carcinogenic risks to humans: Dichloromethane*, IARC, Lyon, France, 2018.
49. C. M. Alder, J. D. Hayler, R. K. Henderson, A. M. Redman, L. Shukla, L. E. Shuster and H. F. Sneddon, *Green Chem.*, 2016, **18**, 3879-3890.
50. K. Alfonsi, J. Colberg, P. J. Dunn, T. Fevig, S. Jennings, T. A. Johnson, H. P. Kleine, C. Knight, M. A. Nagy, D. A. Perry and M. Stefaniak, *Green Chem.*, 2008, **10**, 31-36.
51. D. Prat, A. Wells, J. Hayler, H. Sneddon, C. R. McElroy, S. Abou-Shehada and P. J. Dunn, *Green Chem.*, 2016, **18**, 288-296.
52. F. M. Kerton and R. Marriott, in *Alternative Solvents for Green Chemistry*, The Royal Society of Chemistry, Cambridge, 2nd edn., 2013, pp. 242-261.
53. C. A. Staples, J. B. Williams, G. R. Craig and K. M. Roberts, *Chemosphere*, 2001, **43**, 377-383.
54. C. J. Clarke, W. C. Tu, O. Levers, A. Brohl and J. P. Hallett, *Chem. Rev.*, 2018, **118**, 747-800.
55. M. Labet and W. Thielemans, *Chem. Soc. Rev.*, 2009, **38**, 3484-3504.